IJCRT.ORG ISSN : 2320-2882

INTERNATIONAL JOURNAL OF CREATIVE RESEARCH THOUGHTS (IJCRT)

An International Open Access, Peer-reviewed, Refereed Journal

Assessment Of Toxicological And Biochemical Responses Induced By Biogenic (Green) And Chemical Synthesized Silver Nanoparticles (Ag NPs) On Spawn And Fry Of Indian Major Carp, Rohu, *Labeo rohita*

TOXICOLOGICAL RESPONSES OF AG NPS ON ROHU SPAWN AND FRY

[1] Mayuri Behera, [2] Lopamudra, [3] Sukanta Kumar Nayak

[1]Research Scholar, [2] Research Scholar, [3]Proffessor

[1]Department of Biotechnology,

[1] Maharaja Sriram Chandra Bhanja Deo University, Baripada, India

Abstract: The wide application of silver nanoparticles (Ag-NPs) has led to their significant environmental release, posing substantial ecotoxicological concerns for aquatic ecosystems. While the toxicity of chemically synthesized Ag-NPs (C-Ag-NPs) to freshwater fish, is well-established, the comparative toxicological implications of biogenic (green) synthesized Ag-NPs (G-Ag NPs) remain largely unexplored. This study aimed to assess and compare the dose- and time-dependent toxicity of C-Ag-NPs and G-Ag-NPs on the early life stages (spawn and fry) of the Indian major carp, rohu, *Labeo rohita*. Ag-NPs were synthesized by both chemical and green route method by using the leaf extract of *Clitoria ternatea* and characterized by UV-Vis spectroscopy (peak at 425 nm for both Ag-NPs), SEM (nanostructured, irregular shape), XRD (face-centered cubic crystalline structure), and FTIR (organic capping agents). The C-Ag-NPs and G-Ag-NPs when treated at varied concentrations of both Ag-NPs ranging from 0.01 mg/L to 1000 mg/L through water treatment with rohu spawn (24 hrs) and fry (7 days), demonstrated dose- and time-dependent mortality. 100% mortality of rohu spawn and fry was observed at higher concentrations (500-1000 mg/L) in both the Ag-NPs treatment groups. The C-Ag-NPs exhibited higher toxicity to rohu spawn at concentrations of 10 mg/L to 100 mg/L. Similarly, both types of Ag-NPs induced dose and time dependent oxidative stress with reduced liver GSH and increased lipid peroxidase activity in rohu fry. However, among the two types of AG-NPs, G-Ag-NPs resulted less lipid peroxidase activity and GSH depletion compared to C-Ag-NPs, suggesting a possible mitigated oxidative burden in fish. These findings underscore the significant ecotoxicological threat posed by Ag-NPs to aquatic life, particularly at early developmental stages.

Index Terms - Silver Nanoparticles (Ag-NPs), Toxicity, *Labeo rohita*, Indian major carp, Spawn, Fry, Biogenic, Oxidative Stress, Glutathione (GSH), Lipid Peroxidation (LPX), Malondialdehyde (MDA)

1. INTRODUCTION

The advent of metal and metal oxide nanomaterials has profoundly influenced diverse fields since their discovery, owing to their unique physiochemical properties (Iravani, 2011). Among these, silver nanoparticles (Ag-NPs) have garnered significant attention, finding extensive applications across medical devices, biomedical products, cosmetic formulations, the textile industry, food processing and preservation, functionalized plastics, catalysis (fuel and solar cell construction), electronics, chemical sensing and imaging, biosensors, light trapping, and various consumer products such as washing machines, detergents, paints, and

water filters (Benn and Westerhoff, 2008; Fayaz *et al*., 2009; Naganthran *et al*., 2022; Pasparakis 2022; Abbas *et al*., 2024).

However, the increased production and consumption of Ag-NPs containing products inevitably lead to their release into the environment, particularly aquatic ecosystems, raising significant ecotoxicological concerns. Previous studies have demonstrated the adverse responses induced by various metal and metal oxide NPs (Bi *et al*., 2023) and Ag-NPs being no exception. Over the years, a substantial increase in Ag-NPs utilization has been recorded not only in industrial and biomedical sectors but also in agricultural and aquaculture practices. Consequently, a growing body of literature highlighted the established toxicity of Ag-NPs (Kakakhel *et al*., 2021). Specifically, the toxicological and pathological impacts of waterborne chemically synthesized Ag NPs have well-documented in various freshwater fish species (Ostaszewska *et al*., 2018). Furthermore, evidences also suggest the possible trophic transfer of Ag-NPs through various food chains directly or indirectly which in turn can adversely affect higher trophic levels, including animals and humans (Dang *et al*., 2021).

It's a matter of fact that wise spread applications of nanoproducts synthesized through hazardous chemicals inevitably lead to their discharge into aquatic environments, posing a significant threat to the health and biodiversity of aquatic ecosystems. On the contrary, the toxicological implications of biogenic Ag-NPs especially green route synthesized (G-Ag-NPs) remain largely unclear. Considering the fact that biological materials possess natural content of capping and reducing agents, the biogenic NPs offer numerous advantages such as cost-effective, relatively safer, eco-friendly and stable (Mittal *et al*., 2013; Khodashenas and Ghorbani, 2019; Hamidi *et al*., 2019; Awwad *et al*., 2020; Bandeira *et al*., 2020). Therefore, the present investigation was conducted to evaluate the toxicological and biochemical responses induced by G-Ag-NPs and C-Ag-NPs at the early stages (spawn and fry) of Indian major carp, Rohu (*Labeo rohita* Ham.).

2. Materials and Methods:

2.1. Chemical synthesis of Silver Nanoparticles (C-Ag-NPs)

Ag-NPs was synthesized by chemical method as per the procedure of Dasaradhudu & Srinivasan, (2020), with slight modifications. Briefly, to a 50 ml boiled silver nitrate ($AgNO_3$) (0.003M) solution, 5ml of 1% tri sodium citrate was added drop wise. The mixture was then kept in magnetic stirrer and mixed vigorously at 50-60 ^{0}C until the colour of the solution mixture changed to deep yellowish brown. The solution mixture was then dried and calcinated in *muffle furnace* at 500 ^{0}C for 2 hrs. The resultant powder was collected and processed for further characterization.

2.2. Biogenic synthesis of Silver Nanoparticles (G-Ag-NPs)

G-Ag-NPs was synthesized by using the leaf extract of *C. ternatea* as per the procedure of Krithiga *et al*., (2015) with slight modifications. The aqueous leaf extract was prepared by adding 50 gms of freshly collected leaves of *C. ternatea* with 100 ml distilled water at 1:2 ratio and heated at 100 ^{0}C for nearly 1 hr in magnetic stirrer till the colour of the solution changed to light green colour. The solution was then filtered using Whatman No.1 filter paper and stored for further use. After aqueous extract was made, then 50 ml of 0.1M of aqueous solution of $AgNO_3$ was added to 5 ml of leaf extract and kept in magnetic stirrer at room temperature till colour of the solution mixture changes to yellowish brown indicating the formation of Ag-NPs. Finally, the resultant solution was dried at 80 ^{0}C for 12 hrs in a hot air oven and calcinated in muffle furnace at 500 ^{0}C for 2 hrs. The resultant G-Ag-NPs was collected and processed for further characterization.

2.3. Characterization of synthesized Ag-NPs

The following assays were done to characterise both the synthesized Ag-NPs.

2.3.1. UV- Spectroscopy: The optical properties of the synthesized Ag-NPs were analysed by using UV-Vis spectroscopy.

2.3.2. SEM Study: The structural and morphological characterization was done by using JSM- 7600F scanning electron microscope (SEM) with an accelerating voltage between 10 and 20 KV under vacuum conditions.

2.3.3. XRD: X-ray diffraction (XRD) (XPert Pro MPD- PANalytical), with Cu – Kα (λ = 1.54 Å) radiation was used to investigate the crystal structure of laser-generated Ag-NPs with a grazing incidence angle (3^0) in the 2θ range of 32^0-80^0 for NPs in water and 42^0-66^0 for Ag-NPs in acetone.

2.3.4. FTIR: The functional groups of the synthesized Ag-NPs were identified by Fourier Transform Infrared Spectroscopy (FTIR) analysis using Bruker Alpha II (German).

2.4. Experimental Design for *In vivo* Studies

Healthy *Labeo rohita* spawn (approx. 24 hrs post-hatch) and fry (approx. 2-3 cm length) were purchased from a local hatchery at Baisinga, Mayurbhanj, Odisha. The spawn and fry were maintained at Aquatic Animal Laboratory, Department of Biotechnology, MSCB University, Baripada, Odisha. Rohu spawn and fry were kept at glass aquarium with constant aeration and acclimatized to the experimental

conditions in large, continuously aerated holding tanks containing dechlorinated tap water. During the entire period of study, water parameters were monitored daily and were found to be within their permissible limits (Temperature: 29 ± 2^0C, pH: 7.5 ± 0.2, Dissolved Oxygen: 6.0 ± 0.2 mg/L, Alkalinity: 120 ± 0.5 mg/L). Similarly, rohu fry were fed a commercial diet twice daily.

2.5. Effect of synthesized Ag-NPs on *L. rohita* spawn

The effects of chemical and green synthesized Ag-NPs on *L. rohita* spawn was conducted through water treatment method. Nine treatment groups (for each C-AG-NPs and G-AG-NPs) in duplicate set were exposed to different concentrations of Ag-NPs: 0.01, 0.05, 0.1, 1, 10, 50, 100, 500, and 1000 mg/L alongwith control group without any Ag-NPs treatment were made. Approx. 1000 healthy spawn at a density of approximately 1 L of water per 20 spawn were maintained in each glass tank. After Ag-NPs treatment, the mortality in each treatment group was recorded daily and after 72 hrs post treatment the cumulative percent mortality in each group was calculated.

2.6. Effect of synthesized Ag-NPs on *L. rohita* fry

The effects of synthesized Ag-NPs on *L. rohita* fry was also studied through water treatment method as done in spawn experiment. Nine treatment groups (for each C-AG-NPs and G-AG-NPs) in duplicate set were exposed to different concentrations of Ag-NPs: 0.01, 0.05, 0.1, 1, 10, 50, 100, 500, and 1000 mg/L alongwith control group without any Ag-NPs treatment were made. Healthy rohu fry (100 Nos) was distributed in each tank at a density of approximately 2 L water per 20 fry. After 5 days of acclimatisation, the fry were separately exposed to both the Ag-NPs at varied concentrations ranging from 0.01, 0.05, 0.1, 1, 10, 50, 100, 500, and 1000 mg/L. The mortality in each group was recorded up to 7 days post treatment. Finally, the cumulative percent mortality was calculated in each group. Similarly, 10 fry from each treatment group were collected at 3rd, 5th and 7th days post treatment, to estimate the oxidative stress biomarkers such as lipid peroxidation (LPX) and reduced glutathione (GSH).

2.7. Estimation of Biochemical Parameters

2.7.1. Sample Preparation

Rohu fry (10 Nos) were collected in sterile vials from each treatment group at 3rd, 5th and 7th days post treatment and then sacrificed using an overdose of MS-222 and rinsed in deionized water. 10% (w/v) whole body homogenate was prepared by triturating all fry in ice-cold 50 mM phosphate-buffered saline (PBS, pH 7.2). The homogenate was then centrifuged at 10,000 × rpm for 15 min at 4 ^{0}C. The resulting supernatant was used for tissue biochemical parameters study.

2.7.2. Lipid peroxidation (LPX) Assay

The lipid peroxidation (LPX) assay was performed using the method of Ohkawa *et al*. (1979) with slight modifications. Briefly, 0.1 ml of whole body homogenate was mixed with a TBA reagent containing 0.2 ml of 8.1% sodium dodecyl sulfate, 1.5 ml of 20% acetic acid (pH 3.5), 1.5 ml of 0.8% Thiobarbituric acid (TBA) and 0.8 ml of distilled water. The suspension was then kept in a water bath at 95 ^{0}C for 15 min. The samples were then cooled and centrifuged at 3000 × rpm for 10 min at 4^{0}C. The absorbance of the supernatant was measured at 535nm in a spectrophotometer. The concentration of MDA in each sample was calculated using the standard curve, which was plotted with the absorbance of known MDA standards. The mean (± SD) LPX concentration in each group was expressed as nanomoles of MDA per milligram of protein (nmol MDA/mg protein).

2.7.3. Reduced Glutathione (GSH) Assay

Reduced glutathione (GSH) level in the whole body homogenate was estimated using a spectrophotometric method based on its reaction with 5,5'-dithiobis-(2-nitrobenzoic acid) (DTNB), according to the method of Ellman (1959). The homogenate was centrifuged at 4000 × rpm for 10 min at 4 ^{0}C. Then, 0.5 ml of the supernatant was collected, and 0.5 ml of 10% trichloroacetic acid (TCA) solution was added to it. This mixture was vortexed and then centrifuged at 10,000 × rpm for 10 min at 4 ^{0}C. 0.5 ml of the supernatant was then mixed with 2.5 ml of a 1 mM DTNB solution (prepared in 0.1 M phosphate buffer, pH 8.0). Finally, the mixture was incubated at room temperature for 5 min. After incubation, the absorbance was measured at 412 nm using a spectrophotometer against a blank containing 0.5 ml of 10% TCA and 2.5 ml of 1 mM DTNB solution. The concentration of GSH in each sample was determined using a standard curve of known GSH concentrations. The mean (± SD) GSH content in each Ag-NPs treatment group was expressed as micromoles of GSH per milligram of protein (µmol GSH/mg protein).

2.8. Statistical Analysis

All the data were statistically analysed by two-way analysis of variance (ANOVA) to determine the significant differences at $P < 0.05$ in the mean ± standard deviation (SD) of cumulative percentage of rohu spawn and fry mortality along with the LPX and GSH levels of rohu fry treated with various concentrations of C-Ag-NPs and G-Ag-NPs with that of control groups according to Tukey's HSD.

3. Result

In the present study, Ag-NPs were synthesized both by chemical and green route method. The colour of the $AgNO_3$ salt and reductant mixture solution changed to light yellowish brown within 2 hrs in the C-Ag-NPs (Fig. 1a). Similarly, the change in colour of the $AgNO_3$ salt and leaf extract mixture changed to deep brownish yellow for G-Ag NPs indicating the synthesis of Ag-NPs (Fig. 1b).

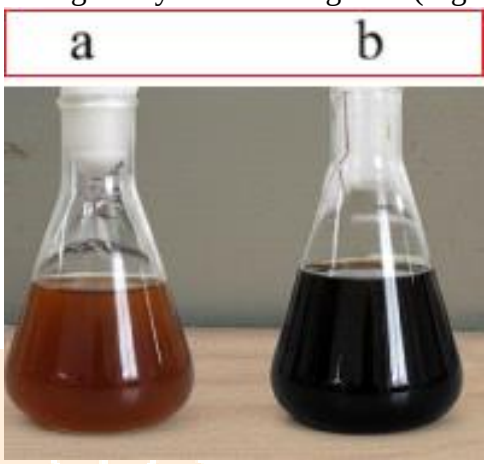

[Fig.1. The change in $AgNO_3$ salt solution to (a) light yellowish brown indicates the synthesis of Ag-NPs by chemical method and to (b) deep brownish yellow colour indicates the biogenic method using the leaf extract of *C. ternatea*]

3.1. Characterization of synthesized NPs

The C-Ag-NPs and G-Ag-NPs were preliminary characterized by UV–visible spectroscopy. The UV spectral analysis of C-Ag-NPs and G-Ag-NPs showed a peak value at 425nm (Fig. 2a & b).

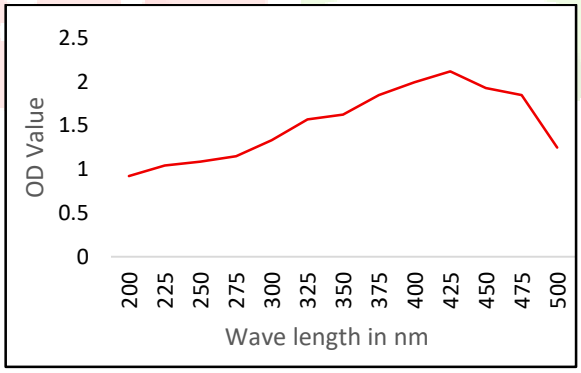

[Fig 2a: UV-Visible spectrophotometric analysis C-Ag-NPs]

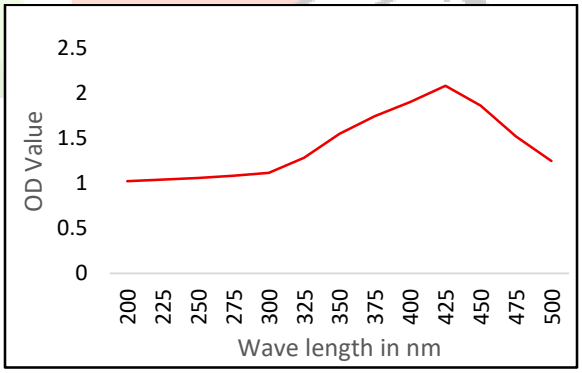

[Fig 2b: UV-Visible spectrophotometric analysis G-Ag-NPs]

The SEM image of C-Ag NPs showed particles with nanostructured morphology composed of a very large number of extremely small, roughly spherical Ag-NPs (Fig. 3a). These NPs are not evenly dispersed but are clustered together, forming highly porous, irregular aggregates. On the other hand, the SEM image of G-Ag-NPs showed particles with diverse morphological features including various irregular shapes, such as cubic-like, rounded, and sharp-edged structures (Fig. 3b). The particles appeared to be densely packed and exhibited some degree of agglomeration, forming larger clusters. The overall morphology indicated a polycrystalline material with a wide distribution of particle sizes and shapes.

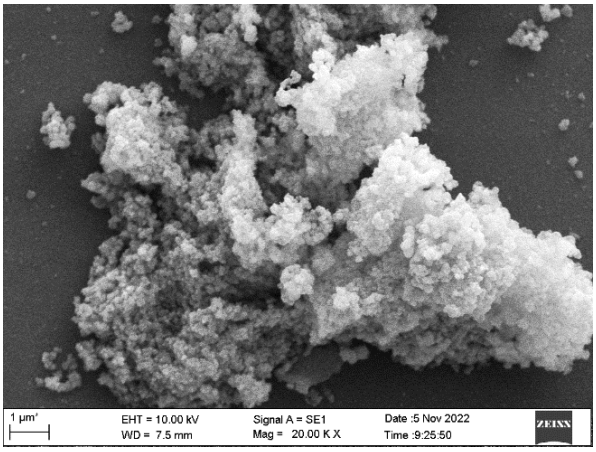

[Fig 3a: Scanning Electron Microscopy image showing porous structure of the synthesized C-Ag-NPs]

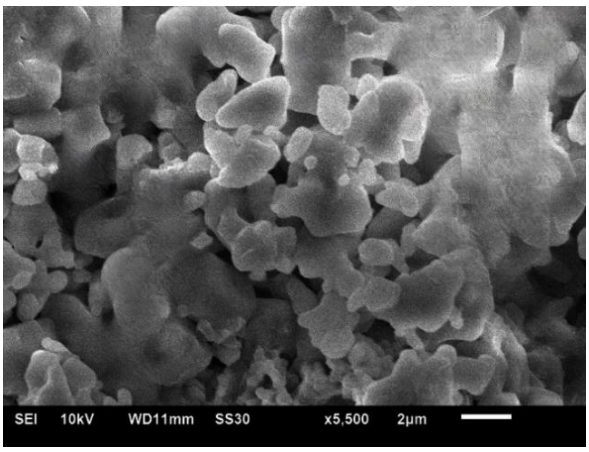

[Fig 3b: Scanning Electron Microscopy image showing the irregular shapes of the synthesized G-Ag-NPs]

The XRD pattern of C-Ag-NPs was consistent with the presence of crystalline Ag-NPs having a face-centered cubic structure. The distinct peaks at approximately 38^0, $44\text{-}45^0$, $64\text{-}65^0$ and $77\text{-}78^0$ (Fig. 4a) correspond to the characteristic planes of metallic silver and possess the expected crystalline structure of (~33.62 nm). Similarly, the XRD pattern of the G-Ag-NPs exhibited several sharp and intense peaks, which confirms the highly crystalline nature of the synthesized material (Fig. 4a). The four main diffraction peaks were located at approximately 2θ values of 38.2^0, 44.3^0, 64.5^0, and 77.4^0. These peaks were indexed to the (111), (200), (220), and (311) planes of face-cantered cubic (FCC) silver (Ag). This indicated that the successful synthesis of G-Ag-NPs and possess the expected crystalline structure of (~28.02 nm).

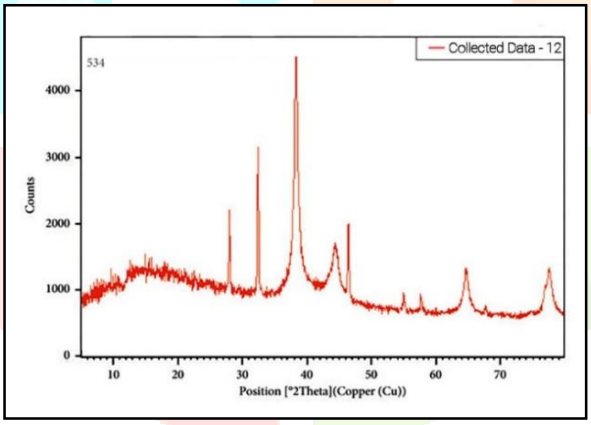

[Fig 4a: XRD pattern showing the crystalline and face-centered cubic structure of the synthesized C-Ag-NPs]

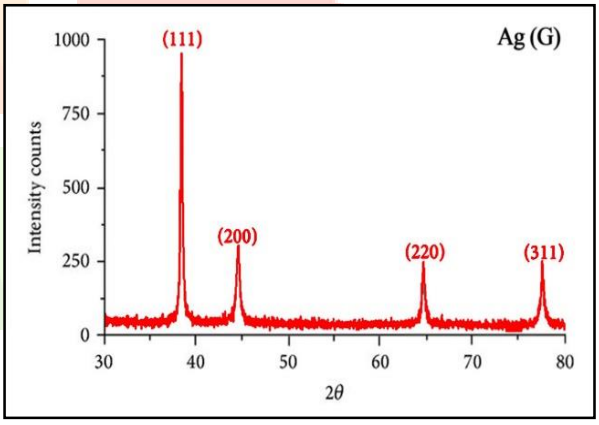

[Fig 4b: XRD pattern showing crystalline structure with sharp and intense peaks of G-Ag-NPs]

Th ıroad a n of 3400-3200 cm^{-1}, which corresponded to the stretching vibrations of O-H (hydroxyl) and N-H (amine) groups (Fig. 5a). This indicated the presence of alcohols, phenols, or amines. Peak at 2925 cm^{-1} was attributed to the symmetric and asymmetric stretching vibrations of C-H bonds, confirming the presence of aliphatic groups in the sample. A strong band at 1640 cm^{-1} was characteristic of the stretching vibration of C=O (carbonyl) bonds, often found in amides and ketones, or C=C stretching of an aromatic ring. The peaks in the range of 1400-1000 cm^{-1} were characteristic of the "fingerprint region," where complex vibrations occurred. A peak at 1372 cm−1 was likely due to the stretching of C-N bonds of amides. Additional absorption bands were observed at 1081 cm^{-1} and 1043 cm^{-1}, which were assigned to the stretching vibrations of C-O bonds from alcohols, ethers, or carboxylic acids. The FTIR results of G-Ag-NPs confirmed that the synthesized G-Ag-NPs were capped by biomolecules containing hydroxyl, amine, carboxyl, and other organic functional groups. These groups likely stabilized the Ag-NPs, preventing their aggregation. On the other hand, a peak at 3265 cm^{-1} corresponded to the stretching vibrations of N-H or O-H bonds, indicating the presence of amines or hydroxyl groups from biomolecules was observed for G-Ag-NPs (Fig. 5b). A weak peak at 3003 cm^{-1} was attributed to the aromatic C-H stretching vibration. A strong, prominent peak at 1661 cm^{-1} was characteristic of the stretching vibration of C=O (carbonyl) bonds in amides, or C=C stretching in aromatic compounds. The peak at 1364 cm^{-1} was assigned to the stretching of C-N bonds of amines. The strong peak at 1148 cm^{-1} was attributed to the stretching vibrations of C-O bonds from alcohols, ethers, or esters.

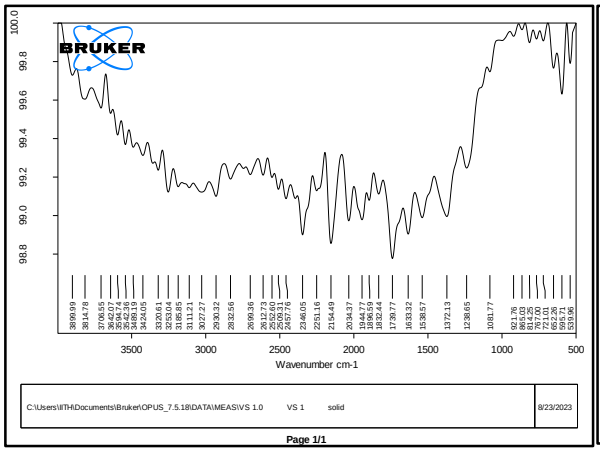

[Fig.5a FTIR analysis showing broad and intense peaks in the region of 3400-3200 cm^{-1} of synthesized C-Ag-NPs]

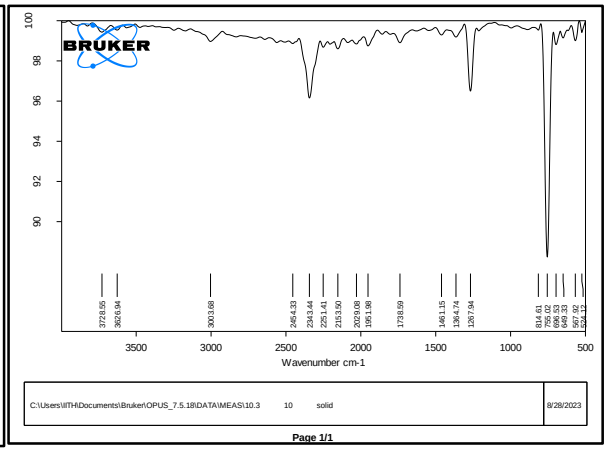

[Fig.5b: FTIR image showing the capped organic functional biomolecules of synthesized G-Ag-NPs]

3.2. Effect of Ag-NPs on rohu spawn and fry: *In vivo* Studies

3.2.1. Effect of Ag-NPs on mortality of rohu spawn

In the present study, both the C-Ag-NPs and G-Ag-NPs were found to exert a dose- and time-dependent toxicity on rohu spawn. The cumulative percentage of mortality of spawn increased with increasing concentrations of Ag-NPs. After 72 hrs of exposure, the cumulative percentage mortality was least (18 ± 0.5) in the 0.01 mg/L treatment group of C-Ag-NPs, whereas in the G-Ag-NPs treatment group, the lowest mortality was observed at the same concentration (12±0.5). The mortality rate increased markedly with higher concentrations. In C-Ag-NPs treated groups, the cumulative mortality was 100% from 50 mg/L to 1000 mg/L concentrations. In contrast, the G-Ag-NPs group exhibited 77.33 (±0.57) mortality at 50 mg/L, while it was 100% at 100 mg/L and above after 72 hrs post treatment. Statistical analysis confirmed significant differences ($P < 0.05$) between C-Ag-NPs and G-Ag-NPs treated groups across most concentrations, indicating that G-Ag-NPs exerted comparatively lower toxicity at intermediate concentrations.

Table 1: The cumulative percent of mortality of rohu (*Labeo rohita*) spawn in C- Ag-NPs and G-Ag-NPs treatment groups after 72hrs

Ag-NPs Type	Concentration of Ag-NPs (mg/L) in different treatment groups									
	0	**0.01**	**0.05**	**0.1**	**1**	**10**	**50**	**100**	**500**	**1000**
C-Ag-NPs	10 ± 0.82^{a}	18 ± 0.5^{b}	56 ± 0.5^{i}	62 ± 0.5^{j}	75 ± 1^{e}	80 ± 0.5^{f}	100^{g}	100^{g}	100^{g}	100^{g}
G-Ag-NPs	10 ± 0.82^{a}	12 ± 0.5^{h}	50 ± 0.5^{c}	59 ± 0.5^{d}	58 ± 0.5^{d}	70 ± 0.5^{k}	77.33 ± 0.57^{l}	100^{g}	100^{g}	100^{g}

[* : Values are expressed as Mean (± SD) of cumulative percentage of mortality. Different superscripts (a–l) indicate significant differences in the cumulative percentage of mortality among various Ag-NPs treatment groups (NP type × concentration) at $P < 0.05$].

3.2.2. Effect of Ag-NPs on mortality of rohu Fry

In the present study, both C-Ag-NPs and G-Ag-NPs exhibited a clear dose and time dependent toxicity on rohu fry. The cumulative percentage mortality increased progressively with increasing concentrations of Ag-NPs after 7 dpt. In the C-Ag-NPs–treated group, the cumulative percentage of mortality was significantly less ($P < 0.05$) in 0.01 mg/L treatment group (30 ± 0.45) as compared to that of G-Ag-NPs. However, cumulative percentage of mortality rose sharply at intermediate concentrations, reaching 48.66 (± 0.20) at 0.05 mg/L and 56.66 (± 0.32) at 0.1 mg/L. At 1 and 10 mg/L, cumulative percentage of mortality was 55.03 (± 0.32) and 70.13 (±0.25), respectively. At higher concentrations, cumulative percentage of mortality was 75.33 (± 0.32) at 50 mg/L and 95.03 (± 0.37) at 100 mg/L, while it was 100% in groups treated with 500 mg/L and 1000 mg/L.

In the G-Ag-NPs–treated group, the lowest cumulative percentage of mortality (25 ±.58) was observed in the control group, which increased significantly ($P < 0.05$) to 34.33 (± 0.38) and 34.66 (± 0.31) at 0.01 and 0.05 mg/L, respectively. The cumulative percentage of mortality increased with higher concentrations, reaching 70.33 (± 0.47) at 10 mg/L and 90 (± 0.7) at 100 mg/L, while it was 100% in groups treated with 500 mg/L and 1000 mg/L. Statistical analysis confirmed significant differences ($P < 0.05$) between Ag-NPs types at lower and intermediate concentrations, with C-Ag-NPs showing higher toxicity at 0.01 mg/L, whereas G-Ag-NPs showed higher mortality at 0.05 - 0.1 mg/L.

Table 2: The cumulative percent of mortality of rohu (*Labeo rohita*) fry in C- Ag-NPs and G-Ag-NPs treatment groups after 7 days post treatment (dpt)

Ag-NPs Type	Concentration of Ag-NPs (mg/L) in different treatment groups									
	0	**0.01**	**0.05**	**0.1**	**1**	**10**	**50**	**100**	**500**	**1000**
C-Ag-NPs	25 ± 4.58^{a}	30 ± 0.45^{i}	48.66 ± 0.2^{d}	56.66 ± 0.32^{j}	55.03 ± 0.32^{j}	70.13 ± 0.25^{e}	75.33 ± 0.32^{f}	95.03 ± 0.37^{k}	100^{h}	100^{h}
G-Ag-NPs	25 ± 4.58^{a}	34.33 ± 0.38^{b}	34.66 ± 0.31^{b}	40.22 ± 0.33^{c}	49.66 ± 0.25^{d}	70.33 ± 0.47^{e}	75 ± 0.36^{f}	90 ± 0.7^{g}	100^{h}	100^{h}

[* : Values are expressed as Mean (± SD) of cumulative percentage of mortality of rohu fry. Different superscripts (a-k) indicate significant differences in the cumulative percentage of mortality among various Ag-NPs treatment groups (NP type × concentration) at $P < 0.05$].

3.2.3. Effect of Ag-NPs on tissue biochemical parameters of rohu fry

3.2.3.1. Effect on LPX content of rohu fry

In the present study, both C-Ag-NPs and G-Ag-NPs were found to exert a dose- and time-dependent increase in liver MDA levels of *L. rohita* fry. At 3 dpt, the MDA level in the control group was least 0.47 (±0.03) nmol/mg protein and significantly increased ($P < 0.05$) with increasing concentrations of both Ag-NPs. In C-Ag-NP-treated groups, MDA reached 4.18 (± 0.67) nmol/mg protein at 500 mg/L, while in G-Ag-NPs treatment group, the increase was less with a mean (±SD) MDA level of 3.67 (± 0.53) nmol/mg protein at the same concentration. The trend persisted with C-Ag-NPs showing a higher induction (4.10 ± 0.58 at 100 mg/L) as compared to that of G-Ag-NPs (3.12 ± 0.34 at 100 mg/L) at 5 dpt. By 7 dpt, MDA levels were further elevated, reaching 4.85 (± 0.99) nmol/mg protein in C-Ag-NPs and 3.75 ± 0.43^{g} nmol/mg protein in G-Ag-NPs at 100 mg/L.

Overall, C-Ag-NPs exhibited significantly higher oxidative stress ($P < 0.05$) compared to G-Ag-NPs at corresponding concentrations across all exposure durations. The lowest MDA levels were consistently observed in the control and 0.01 mg/L groups, while the highest levels were recorded at 500 mg/L for both types of NPs.

Table 3: The mean (± SD) nmol/mg protein of liver MDA levels at different time intervals in rohu (*Labeo rohita*) fry exposed to varying concentrations of C-Ag-NPs and G-Ag-NPs

Day	Ag-NPs Type	Concentration of Ag-NPs (mg/L) in different treatment groups									
		0	**0.01**	**0.05**	**0.1**	**1.0**	**10**	**50**	**100**	**500**	**1000**
3 dpt	C-Ag-NPs	0.47 ± 0.03^{a}	0.50 ± 0.05^{ab}	0.60 ± 0.06^{b}	0.77 ± 0.12^{c}	1.21 ± 0.24^{d}	1.93 ± 0.25^{e}	2.34 ± 0.18^{f}	3.30 ± 0.52^{g}	4.18 ± 0.67^{h}	ND
	G-Ag-NPs	0.47 ± 0.03^{a}	0.46 ± 0.12^{a}	0.45 ± 0.11^{a}	0.69 ± 0.11^{b}	0.89 ± 0.31^{bc}	1.52 ± 0.16^{cd}	1.94 ± 0.33^{d}	2.63 ± 0.19^{e}	3.67 ± 0.53^{f}	ND
5 dpt	C-Ag-NPs	0.45 ± 0.06^{a}	0.47 ± 0.12^{ab}	0.80 ± 0.15^{b}	0.90 ± 0.18^{c}	1.49 ± 0.11^{d}	2.16 ± 0.27^{e}	2.93 ± 0.13^{f}	4.10 ± 0.58^{g}	ND	ND
	G-Ag-NPs	0.45 ± 0.06^{a}	0.48 ± 0.07^{ab}	0.69 ± 0.03^{b}	0.84 ± 0.08^{c}	1.24 ± 0.10^{d}	1.72 ± 0.16^{e}	2.89 ± 0.49^{f}	3.12 ± 0.34^{g}	4.28 ± 0.81^{h}	ND
7 dpt	C-Ag-NPs	0.45 ± 0.05^{a}	0.60 ± 0.07^{b}	0.81 ± 0.16^{c}	1.07± 0.11^{d}	1.74 ± 0.24^{e}	2.64 ± 0.20^{f}	4.07 ± 0.42^{g}	4.85 ± 0.99^{h}	ND	ND
	G-Ag-NPs	0.45 ± 0.05^{a}	0.53 ± 0.07^{ab}	0.67 ± 0.09^{b}	0.86 ± 0.07^{c}	1.26 ± 0.23^{d}	2.31 ± 0.05^{e}	3.11 ± 0.10^{f}	3.75 ± 0.43^{g}	ND	ND

[*: "ND" indicates Not Done due to 100 % rohu fry mortality in that Ag-NPs treatment groups.
**: Values are expressed as Mean (±SD) nmol/mg protein of liver MDA level at different time intervals in rohu (*Labeo rohita*) fry exposed to varying concentrations of C-Ag-NPs and G-Ag-NPs. Different Superscripts indicate statistically significant differences liver MDA levels among concentrations and NPs types at $P < 0.05$]

3.2.3.2. Effect on GSH content of rohu fry

In the present study, both C-Ag-NPs and G-Ag-NPs exhibited a clear dose- and time-dependent depletion of tissue glutathione (GSH) in *L. rohita* spawn. The highest GSH levels were observed in the control and 0.01 mg/L groups, while a significant decline ($P < 0.05$) was recorded with increasing concentrations. On the 3rd day, GSH levels in C-Ag-NPs decreased from 8.24 (± 0.71) nmol/mg protein in control to 3.92 (± 0.24) nmol/mg protein at 500 mg/L, with no detectable GSH at 1000 mg/L. Similarly, in G-Ag-NPs, GSH decreased from 9.01 (± 0.10) nmol/mg protein in control to 4.93 (± 0.16) nmol/mg protein at 500 mg/L, and was undetectable at 1000 mg/L. By the 5th day, the GSH content reduced from 7.99 (± 0.67) nmol/mg protein in control to 4.15 (± 0.10) nmol/mg protein at 100 mg/L, with complete mortality at higher concentrations in C-Ag-NPs. In G-Ag-NPs, GSH declined from 8.48 (± 0.43) nmol/mg protein in control to 2.44 (± 0.68) nmol/mg protein at 500 mg/L, and was 100% mortality at 1000 mg/L. On the 7th day, GSH levels further declined in C-Ag-NPs, values decreased from 7.57 (± 0.11) nmol/mg protein in control to 3.93 (± 0.16) nmol/mg protein at 100 mg/L, with 100% mortality in GSH at higher concentrations. In contrast, G-Ag-NPs showed higher retention, with values reducing from 7.84 (± 0.17) nmol/mg protein in control to 4.07 (± 0.13) nmol/mg protein at 100 mg/L, again with complete loss beyond this dose. Overall, G-Ag-NPs retained significantly higher GSH levels compared to C-Ag-NPs across all exposure periods, indicating that C-Ag-NPs induced stronger oxidative stress in rohu spawn.

Table 4: The mean (± SD) nmol/mg protein of liver glutathione (GSH) levels at different time intervals in rohu (*Labeo rohita*) fry treated with varying concentrations of C-Ag-NPs and G-Ag-NPs

Day	NPs Type	Concentration of Ag-NPs (mg/L) in different treatment groups									
		0	0.01	0.05	0.1	1.0	10	50	100	500	1000
3rd	C-Ag-NPs	8.24± 0.71^{a}	7.80±0.23^{a}	7.11 ±0.13^{b}	6.52± 0.32^{c}	6.21± 0.40^{c}	5.99± 0.15^{c}	5.19± 0.23^{d}	4.53± 0.50^{e}	3.92±0.24^{f}	ND
	G-Ag-NPs	9.01± 0.10^{a}	8.64± 0.25^{a}	7.73 ±0.24^{b}	7.08± 0.40^{c}	6.52± 0.12^{c}	6.29± 0.22^{c}	6.03± 0.09^{c}	5.23± 0.39^{d}	4.93±0.16^{d}	ND
5th	C-Ag-NPs	7.99± 0.67^{a}	7.62± 0.21^{a}	6.72 ±0.38^{b}	6.31± 0.22^{bc}	6.05± 0.07^{bc}	5.39± 0.34^{cd}	5.06± 0.06^{cd}	4.15± 0.10^{e}	ND	ND
	G-Ag-NPs	8.48± 0.43^{a}	7.80± 0.23^{a}	6.88 ±0.38^{b}	6.57± 0.39^{bc}	6.08± 0.07^{c}	5.42± 0.40^{d}	5.04± 0.45^{d}	4.13± 0.10^{e}	2.44±0.68^{f}	ND
7th	C-Ag-NPs	7.57± 0.11^{a}	7.13± 0.06^{ab}	6.23 ±0.20^{c}	6.05± 0.04^{c}	5.55± 0.18^{d}	5.06± 0.06^{e}	4.88± 0.19^{e}	3.93± 0.16^{f}	ND	ND
	G-Ag-NPs	7.84± 0.17^{a}	7.31± 0.15^{ab}	6.79 ±0.47^{b}	6.28± 0.15^{c}	5.84± 0.34^{d}	5.28± 0.31^{e}	4.91± 0.31^{e}	4.07± 0.13^{f}	ND	ND

[*: "ND" indicates Not Done due to 100% mortality in the specified Ag-NPs treatment groups.
**: Values are expressed as Mean (±SD) nmol/mg protein of GSH level in rohu (*Labeo rohita*) fry exposed to varying concentrations of C-Ag-NPs and G-Ag-NPs at different time intervals. Different Superscripts indicate statistically significant differences in the GSH level among concentrations and NPs types at $P < 0.05$]

4. Discussion

Now-a-days, the increasing utilization of Ag-NPs across industrial, biomedical, agricultural, and aquacultural sectors inevitably leads to the contamination of aquatic environments, posing a significant threat to aquatic ecosystem health and biodiversity (Wasmuth *et al*., 2016). Therefore, the present investigation carried out to study the ~~eco~~toxicological effects of Ag-NPs synthesized chemically and green route method on early life stages (spawn and fry) of the Indian major carp, *L. rohita*.

Earlier several researchers have successfully synthesized Ag-NPs chemically and biogenic methods. In this study we have also synthesized Ag-NPs chemically as well as by using leaf extract of *C. ternatea*. While, earlier several researchers have successfully synthesized Ag-NPs and /or dopped Ag-NPs by utilising Leaves, flowers, root and even whole plant extracts of *C. ternatea*, many researchers have also documented promising antimicrobial activity, insecticidal activity, biofilm preventing, cytotoxicity against cancer cells etc (Singh *et al*., 2025; Madhumitha, *et al*., 2023; Varadavenkatesan, *et al*., 2020; Malabadi, *et al*., 2012 & 2015; Krithiga, *et al*., 2015; Vanaraj *et al*., 2017; Fatimah *et al*., 2020; Citradewi *et al*., 2021; Lall *et al*., 2021).

The characterisation studies confirmed the successful synthesis of Ag-NPs and were in agreement with the findings of previous researchers. UV-Vis spectra for both C-Ag-NPs and G-Ag-NPs showed a characteristic surface plasmon resonance (SPR) peak at 425 nm, which is consistent with previous studies on Ag-NPs (Vasantyh *et al*., 2018). However, distinct morphological differences could be observed in the synthesized Ag-NPs. The SEM analysis showed that C-Ag-NPs were porous, spherical with agglomeration while the G-Ag-NPs exhibited a more diverse morphology with irregular shapes and a higher degree of agglomeration.

The XRD patterns confirmed the crystalline, face-centered cubic structure of both types of Ag-NPs, a well-known characteristic of metallic silver. The presence of a broader background signal in the G-Ag-NPs is indicative of amorphous organic matter from the plant extract, a common finding in green synthesis (Iravani *et al*., 2014). The XRD pattern of the C-Ag-NPs exhibited several sharp and intense peaks, which confirms the highly crystalline nature of the synthesized material. The narrowness of the peaks (38.2^0, 44.3^0, 64.5^0, and 77.4^0) indicated a good degree of crystallinity and a relatively large crystallite size for the NPs- write in discussion. Similarly, the XRD pattern of G-Ag-NPs is consistent with the presence of crystalline Ag-NPs

having a face-centred cubic structure. The distinct peaks at approximately 38^0, 44-45^0, 64-65^0 and 77-78^0 correspond to the characteristic planes of metallic silver. The broader background signal might indicate the presence of amorphous organic material which is commonly observed in green-synthesized Ag-NPs due to the involvement of biomolecules as reducing and capping agents. This characterization is crucial for confirming the successful synthesis and crystalline nature of the Ag-NPs. The XRD pattern indicated the successful synthesis of the crystalline structure with a size of ~33.62 nm for C-AG-NPS WHILE THAT OF G-AG-NPS WAS FOUND TO BE ~28.02 nm.

This is further supported by the FTIR analysis showed a variety of functional groups (O-H, N-H, C=O, C-O) in both types of Ag-NPs, confirming the role of biomolecules as capping and stabilizing agents, particularly for the G-Ag-NPs (Vasanth and Kurian, 2017). The FTIR analysis of C-Ag-NPs showed a broad and intense peak was present in the region of 3400-3200 cm^{-1}, which corresponded to the stretching vibrations of O-H (hydroxyl) and N-H (amine) groups. This indicated the presence of alcohols, phenols, or amines. Assigned to the stretching vibrations of C-O bonds from alcohols, ethers, or carboxylic acids. The FTIR results confirmed that the synthesized Ag-NPs were capped by biomolecules containing hydroxyl, amine, carboxyl, and other organic functional groups. These groups likely stabilized the NPs, preventing their aggregation. On the other hand, a peak at 3265 cm^{-1} corresponded to the stretching vibrations of N-H or O-H bonds, indicating the presence of amines or hydroxyl groups from biomolecules was observed for G-Ag-NPs. The presence of these functional groups indicated that the biomolecules used in the synthesis were effectively bound to the surface of the Ag-NPs, where they acted as both reducing and capping agents, providing colloidal stability to the nanoparticles.

Nanotoxicity is an issue associated with different nanomaterials. Over the years such type of metal and metal oxide including AG-NPs induced toxicity are demonstrated in a wide range of fish species (Khan *et al*., 2015; Du *et al*., 2018). Earlier several researchers have studied the adverse effect of Ag-NPs in aquatic environment and aquatic organisms like fish (Asharani *et al*., 2008; Yeo and Kang 2008; Bilberg *et al*., 2010; Powers *et al*., 2010; Wu *et al*., 2010). Our findings also indicated a dose and time-dependent toxicity of both C-Ag-NPs and G-Ag-NPs, as evidenced by significant mortality and alterations in key oxidative stress biomarkers, specifically liver glutathione (GSH) and lipid peroxidation (LPX). Mortality data revealed that even low concentrations (e.g., 0.01 mg/L) of both Ag-NPs caused significant mortality over time. The high mortality at higher concentrations (100% mortality at a concentration 500 mg/L and above) is a clear indication of their acute toxicity, aligning with findings in other freshwater fish species.

At a biochemical level, the toxicity is clearly mediated by oxidative stress. The liver MDA data showed a consistent and significant increase in lipid peroxidation, a key biomarker for cell membrane damage. Conversely, the liver GSH levels were depleted, reflecting the exhaustion of the antioxidant system as the fish attempted to counteract the oxidative damage. These findings corroborate the established mechanism of Ag-NPs toxicity, where the Ag-NPs, or the Ag^+ ions they release, generate an excess of reactive oxygen species that overwhelms the cellular antioxidant defences (Ghannam *et al*, 2025; Shokouhi *et al*., 2023).

Earlier Rajkumar *et al*. (2015) also demonstrated the dose dependent toxicity in *L. rohita* by chemical synthesized Ag-NPs. They have recorded that C-Ag-NPs at 500 mg kg^{-1} lead to 100% mortality and 50% mortality at 100 mg kg^{-1} in *L. rohita*. In the present study, while both were ultimately toxic, the C-Ag-NPs generally exhibited greater toxicity than the G-Ag-NPs. For instance, at 10 mg/L and Day 3, the C-Ag-NPs caused 40% mortality in fry compared to 30.04% for G-Ag-NPs. This disparity is also reflected in the MDA and GSH data; the green synthesized NPs consistently resulted in lower MDA levels and higher GSH levels than their chemical counterparts. This is likely due to the presence of a natural capping layer of biomolecules on the G-Ag-NPs, which may reduce the release of toxic silver ions into the water, thereby reducing their bioavailability and mitigating their toxic effects. This inherent advantage of green-synthesized nanoparticles underscores the potential for developing safer and more environmentally friendly nanomaterials (Vasanth and Kurian, 2017). However, the high mortality observed in both groups at higher concentrations (≥ 500 mg/L), indicates that even the "safer" green route does not fully eliminate the lethal effects of these nanoparticles at elevated levels. This study therefore confirmed the significant toxicological threat posed by both the Ag-NPs in fish in early developmental stages.

5. Conclusion

The present study provides clear evidence that both chemically synthesized and green-synthesized Ag-NPs induced dose- and time-dependent toxicological effects in *L. rohita* spawn and fry. The C-Ag-NPs caused significantly higher mortality and oxidative stress responses compared to G-Ag-NPs, as reflected by elevated lipid peroxidation and greater glutathione depletion. Although, G-Ag-NPs exhibited relatively less toxic at intermediate concentrations, at higher concentrations, both types of Ag-NPs are toxic. Therefore, both forms of Ag-NPs pose significant ecotoxicological risks to aquatic organisms at elevated concentrations.

6. Acknowledgement

Authors are thankful to the Vice Chancellor, Maharaja Sriram Chandra Bhanja Deo University (Erstwhile North Orissa University) and Head, Department of Biotechnology, MSCB University, Baripada, Odisha, India for providing necessary permission and facilities to carry out the present investigation which is a part of Ph. D research of Ms. M. Behera and Mrs Lopamaudra.

7. Author's contributions

S. K. Nayak : Supervisor. Designed the study, and finalize the MS

Mayuri Behera and Lopamudra : Contributed equally for the present Investigation by conducting all the experiments, analyzed data and prepared the draft copy of the MS

Funding **: None**

Ethics approval **: As per the ethical approval of the University**

Ethical Statement **:** The present study involving toxicological studies in spawn and fry experiments was conducted as per the guidelines and approval of the ethical committee of the University.

References

[1] Abbas, R.; Luo, J.; Qi, X.; Naz, A.; Khan, I.A.; Liu, H.; Yu, S.; and Wei, J., 2024. Silver Nanoparticles: Synthesis, Structure, Properties and Applications. *Nanomaterials*, 14, 1425.

[2] Asharani P.V., Wu Y.L., Gong Z., Valiyaveetti S. 2008. Toxicity of silver nanoparticles in zebrafish models. *Nanotechnology* 1925. 55-102.

[3] Benn, T.M. and Westerhoff, P. 2008. Nanoparticle Silver Released into Water from Commercially Available Sock Fabrics. *Environmental Science & Technology*, 42, 4133-4139.

[4] Bilberg K., Doving K.B., Beedholm K. and Baatrup E., 2011. Silver nanoparticles disrupt olfaction in Crucian carp *Carassius carassius*) and Eurasian perch *Perca fluviatilis*). *Aquatic Toxicology*, 104, 145–152.

[5] Citradewi P.W., Hidayat H., Purwiandono G. and Fatimah I., 2021. *Clitorea ternatea*-mediated Silver Nanoparticle-doped Hydroxyapatite Derived from Cockle shell as Antibacterial Material. *Chemical Physics Letters* 769, 138412.

[6] Cushen M., Kerry J., Morris M., Cruz-Romero M., and Cummins, E. 2012. Nanotechnologies in the food industry – Recent developments, risks and regulation, *Trends in Food Science & Technology*, 24, 30-46.

[7] Dang F., Huang Y., Wang Y. and Zhou D. 2021.Transfer and toxicity of silver nanoparticles in the food chain, *Environmental Science. Nano*. 6, 2955.

[8] Dasaradhudu Y. and Srinivasan M. A., 2020. Synthesis and characterization of silver nano particles using co-precipitation method, *Materials Today*, 720-723

[9] Ellman, G. L. 1959. Tissue sulfhydryl groups. *Archives of Biochemistry and Biophysics*, 82(1): 70-77.

[10] Fatimah I., Hidayat H., Nugroho B., and Husein S., 2020. Ultrasound-assisted biosynthesis of silver and gold nanoparticles using Clitoria ternatea flower. *South African Journal of Chemical Engineering* 34: 97-106.

[11] Fayaz A. M., Balaji K., Kalaichelvan P. T., and Venkataraman R. 2009). Fungal based synthesis of silver nanoparticles-An effect of temperature on the size of particles, *Colloids and Surfaces B: Biointerfaces*, 74,123–126.

[12] Ghannam H. E, Khedr A. I., El-Sayed R., Ahmed N. M., and Salaah S. M, 2025. Oxidative stress responses and histological changes in the liver of Nile tilapia exposed to silver bulk and nanoparticles. *Scientific Reports*, 151:15390.

[13] Iravani S. 2011. Green Synthesis of metal nanoparticles using plants. Green Chemistry, 13, 2638-2650.

[14] Iravani S., Korbekandi H., Mirmohammadi S.V. and Zolfaghari B. 2014 Synthesis of Silver Nanoparticles: Chemical, Physical and Biological Methods. *Research in Pharmaceutical Sciences*, 9, 385-406.

[15] Kakakhel M. A., Wu F., Feng H., and Hassan Z., 2021. Biological synthesis of silver nanoparticles using animal blood, their preventive efficiency of bacterial species, and ecotoxicity in common carp fish, *Microscopy Research and Technique*,84(8):1765-1774.
[16] Khalil M.M.H., Ismail E.H., El-Baghdady K.Z., and Mohamed D., 2013. Green synthesis of silver nanoparticles using olive leaf extract and its antibacterial activity. Arabian Journal of Chemistry, 7(6): 1131-1139.
[17] Khan, M. S., Jabeen, F., Qureshi, N. A., Asghar, M. S., Shakeel, M., and Noureen, A. 2015. Toxicity of silver nanoparticles in fish: a critical review. *J Bio Environ Sci*, 6(5): 211-227.
[18] Khodashenas, B., and Ghorbani, H. R. 2019). Synthesis of silver nanoparticles with different shapes, *Arabian Journal of Chemistry*, 12(8): 1823-1838.
[19] Krithiga N., Rajalakshmi A., and Jayachitra, A. 2015. Green Synthesis of Silver Nanoparticles Using Leaf Extracts of Clitoria ternatea and Solanum nigrum and Study of Its Antibacterial Effect against Common Nosocomial Pathogens, *Journal of Nanoscience*, 928204.
[20] Krithiga N., Rajalakshmi A., and Jayachitra A., 2015. Green Synthesis of Silver Nanoparticles Using Leaf Extracts of Clitoria ternatea and Solanum nigrum and Study of Its Antibacterial Effect against Common Nosocomial Pathogens. *Journal of Nanomaterials*, 1-7.
[21] Lall, Y., Samal, R. R., Sagar, S. K., and Kumar, S. 2021. Formulation of Clitoria ternatea Leaves-mediated Silver Nanoparticles to Control Aedes aegypti Larvae, *Journal of Communicable Diseases*, 53(3): 190-200.
[22] Madhumitha, H., Ranjani, S., Karunyaa, J. R., and Hemalatha, S. 2023. Clitoria Ternatea Floral Mediated Synthesis, Characterization, Antioxidant, and Cytotoxicity Evaluation of Silver Nanoparticles: Clitoria ternatea floral mediated SNP to control BC. *Archives of Breast Cancer*, 222-231.
[23] Malabadi, R. B., Naik, S. L., Meti, N. T., Mulgund, G. S., Nataraja, K., and Kumar, S. V. 2012. Silver nanoparticles synthesized by in vitro derived plants and callus cultures of Clitoria ternatea; Evaluation of antimicrobial activity. *Research in Biotechnology*, *3*, 5.
[24] Mittal, A. K., Chisti, Y., and Banerjee, U. C. 2013. Synthesis of metallic nanoparticles using plant extracts. *Biotechnology Advances*, 31(2): 346-56.
[25] Naganthran A., Verasoundarapandian G., Khalid, F.E., Masarudin, M.J., Zulkharnain, A., Nawawi, N.M., Karim, M., Che Abdullah, C.A., and Ahmad, S.A., 2022. Synthesis, characterization and biomedical application of silver nanoparticles. *Materials*, *15*, 427
[26] Ohkawa, H., Ohishi, N., and Yagi, K. 1979. Assay for lipid peroxides in animal tissues by thiobarbituric acid reaction. *Analytical Biochemistry*, 95(2): 351–358.
[27] Ostaszewska T., Sliwinski J., Kamaszewski M., Sysa P. and Chojnacki M., 2018. Cytotoxicity of silver and copper nanoparticles on rainbow trout *Oncorhynchus mykiss*) hepatocytes. *Environ Sci Pollut Res*, 25: 908–915.
[28] Pasparakis, G. 2022. Recent developments in the use of gold and silver nanoparticles in biomedicine. *Wiley interdisciplinary reviews: Nanomedicine and nanobiotechnology*, *14(*5): e1817.
[29] Powers C.M., Yen J., Linney E.A., Seidler F.J. and Slotkin T.A. 2010. Silver exposure in developing Zebrafish *Danio rerio*): Persistent effects on larval behavior and survival. Neurotoxicology and Teratology 32(3): 391-397.
[30] Rajkumar K.S., Kanipandian N. and Thirumurugan R., 2015. Toxicity assessment on haemotology, biochemical and histopathological alterations of silver nanoparticles-exposed freshwater fish *Labeo rohita*. *Applied Nanoscience*, 6(1): 19-29.
[31] Shokouhi J., Askary Sary A., Chelemal Dezfoulnejad M., Khodadadi M. and Masoomizadeh S.Z. 2023. Effect of a long-time exposure of green and chemical synthesized silver nanoparticles on antioxidant defense system and immune response in Asian seabass Lates calcarifer). Iranian Journal of Fisheries Sciences, 24(2): 259-275.
[32] Singh S. R., Kittur B., Bhavi S. M., Thokchom, Padti A. C., Bhat S. S., Bajire S. K., Shastry R. P., Srinath B.S., Sillanpaa M., Harini B.P. and Yarajarla R. B.., 2025 The effect of Clitoria ternatea L. flowers-derived silver nanoparticles on A549 and L-132 human cell lines and their antibacterial efficacy in Caenorhabditis elegans in vivo. *Hybrid Advances*, 8,100359.
[33] Vali S., Majidiyan N., Yalsuyi A.M., Vajargah M.F., Prokic M.D. and Faggio C. 2022. Ecotoxicological Effects of Silver Nanoparticles Ag-NPs) on Parturition Time, Survival Rate, Reproductive Success and Blood Parameters of Adult Common Molly *Poecilia sphenops*) and Their Larvae. *Water*, 14(2): 144.
[34] Vanaraj S., Keerthana B. B., and Preethi, K. 2017. Biosynthesis, characterization of silver nanoparticles using quercetin from Clitoria ternatea L to enhance toxicity against bacterial biofilm. *Journal of Inorganic and Organometallic Polymers and Materials*, *27(*5): 1412-1422.

[35] Varadavenkatesan T., Vinayagam R., and Selvaraj R. 2020. Green synthesis and structural characterization of silver nanoparticles synthesized using the pod extract of Clitoria ternatea and its application towards dye degradation. *Materials Today: Proceedings, 23*, 27-29.
[36] Vasanth G. and Kurian R. J. 2017. Toxicity evaluation of silver nanoparticles synthesized by chemical and green routes in different experimental models. *Journal of Artificial cells, Nanomedicines and Biotechnology*, 45(8): 1721-1727.
[37] Vasanth S. B. and Kurian G. A.2017 Toxicity evaluation of silver nanoparticles synthesized by chemical and green route in different experimental models, *Artificial Cells, Nanomedicine, and Biotechnology*, 45(8.): 1721-1727.
[38] Wasmuth, S., Pritchard, K., and Kaneshiro, K. 2016. Occupation-Based Intervention for Addictive Disorders: A Systematic Review. *Journal of Substance Abuse Treatment, 58*, 20-30.
[39] Wu Y., Zhoua Q., Li H., Liua W., Wanga T., and Jianga G., 2010. Effects of silver nanoparticles on the development and histopathology biomarkers of Japanese medaka (*Oryzias latipes*) using the partiallife test. Aquatic Toxicology 100(2): 160-167.
[40] Yeo M. and Kang M., 2008. Effects of nanometer sized silver materials on biological toxicity during Zebra fish embryogenesis. *Bulletin of the Korean Chemical Society* 29(6): 1179-1184.